

Urban Heat Island Amplification Estimates on Global Warming Using an Albedo Model

Alec Feinberg, Ph.D., DfRSoft Research

DfRSoft@gmail.com

Vixra: 2003.0088, DOI: 10.13140/RG.2.2.32758.14402/4

Key Words: Urban Heat Islands, Albedo modeling, UHI amplification effects, global warming causes and amplification effects, UHI footprint, UHI heat dome, cool roofs, Sea Ice and moisture feedbacks

Abstract

In this paper we provide nominal and worst case estimates of radiative forcing due to UHI effect (including urban areas) using a Weighted Amplification Albedo Solar Urbanization (WAASU) Model. This is done with the aid of reported findings from UHI footprint and dome studies that simplified estimates for UHI amplification factors. Using this method, we find between 1.6 and 7.5% of global warming may be due to the UHI effect (with urban areas). These values may increase to between 5 and 24% when climate feedbacks are estimated. The model also found that the effect was proportional to the UHI amplification area coverage with area sensitive estimate was about $0.095 (W/m^2)/\%$ Normalized Area. This value would also increase when climate feedbacks are considered. The model is also used to provide an assessment of Sea Ice feedback warming. Results provides insight into the UHI area effects from a new perspective and illustrates that one needs to take into account effective UHI amplification factors when assessing UHI's warming effect on a global scale. Lastly, such effects likely show a more persuasive argument for the need of world-wide UHI albedo goals.

1. Introduction

It is concerning that there are so few UHI publications recently on their possible influences to global warming. Part of the motivation for this paper is to illustrate the continual need for more up-to-date related studies including UHI amplification effects (that include their urban areas) as will be discussed in this paper. The subject of UHI effect having significant contributions to global warming is very important and should remain so. The topic has a controversial history. One such paper, McKittrick and Michaels (2007) found that the net warming bias at the global level may explain as much as half the observed land-based warming. This study was criticized by Schmidt (2009) and defended for a period of about 10 years by McKittrick (see McKittrick Website). Other authors have also found significance (Zhao, 1991; Feddema et al., 2005; Ren et al., 2007, 2008; Jones et al., 2008; Stone, 2009; Zhao, 2011; Yang et al. 2011, and Haung et al. 2015). These studies used land-based temperature station data to make assessments. Although the studies have all found global warming UHI significance with different assessments, they have yet to influence the IPCC enough to necessitate albedo recommendations in their many reports and meetings like the CO₂ effort. This is important because, we feel it is important that the IPCC's be more proactive in this area in helping the global community recognizing the need for UHI albedo guidelines. Although they have provided reports on UHIs including health related issues, the response to their reports does not appear to be effective on the global scale compared with the on-going CO₂ effort.

The contention that UHI effects are basically only of local significance is most likely related to urban area estimates. For example, IPCC (Satterthwaite et. al. 2014) AR5 report references Schneider et al. (2009) study that resulted in urban coverage of 0.148% of the Earth (Table 1). This seemingly small area tends to dismiss the contention that UHI effect can play a large scale role in global warming. Furthermore, estimates of how much of land has been urbanized vary widely in the literature and this is in part due to the definition of what is urban and the datasets used. Although, such estimate are important for environmental studies, obtaining true estimates for the small urbanized area relative to the total land is apparently very difficult. This is compounded by the fact that there is a significant difference in how groups define the term urban. Thus, urbanized surface area land approximations vary widely and most are obtained with satellite measurements sometimes supplemented in some way with census data. Table 1 captures the variations from some papers that are of interest.

In addition, global warming UHI amplification effects have not been quantified to a large degree related to area estimates. Urbanized average solar areas remain unknown.

Table 1. Urbanization area extent estimates from various sources

Percent of Land	Percent of Earth	References
2.7	0.783	GRUMP (2005), using NASA satellite light studies based on 2004 data and supplemented with census data
1%	0.29	NASA (2000) Satellite data, Galka (2016)
0.51	0.148	Schneider et al. (2009), based on 2000-2001 data and referenced in the IPCC report (Satterthwaite, 2014)
0.5%	0.145	Zhou (2015), based on a 2000 data set

In our study, one key paper listed in the table that is studied is due to Schneider et al. (2009) since it is cited by the AR5 2014 IPCC report (Satterthwaite et al. 2014). In Schneider paper, the larger area found in the GRUMP 2005 study in Table 1 is criticized. These area estimates are important in our paper as we are using a *Weighted Amplification Albedo Solar Urbanization (WAASU) Model*. Amplification factors that we will use are related to such urban coverage. Therefore, in this study both the Schneider et al. and GRUMP studies will be used as the nominal and worst cases urbanization area estimates respectively. Furthermore they were both done using data set from around 2000 which is a convenient time to extrapolate down to 1950 and up to 2019 (see Sec. 3).

In our study, where we introduce the WAASU model, we will see that it has some advantages over the ground-based temperature studies like McKittricks and Michaels. The model is non probabilistic, in line with the way typical energy budgets are calculated, it uses only two key parameters (urban coverage, and average albedo). Because it is simplistic, it has transparency compared with the complex land-based studies.

UHI Amplification Effects

The table below lists the global warming causes and amplification effects. In this section we will summarize only the UHI amplification effects listed in the table since the root causes and the main global warming amplification effects are fairly well known.

Table 2. Global Warming Cause and Effects

Global Warming Causes →	Population → Expanding Urban Heat Islands (UHI), Roads & Increases in Greenhouse gas
Global Warming Feedback Amplification Effects →	Water vapor feedback, land albedo due to cities & roads, Ice and snow – albedo feedback, lapse rate feedback, cloud feedback, etc.
Urban Heat Island Amplification Effects →	UHI Solar Heating Area (Building Areas), UHI Building Heat Capacities, Humidity Effects and Hydro-Hotspots, Reduced Wind Cooling, Solar Canyons, Loss of Wetlands, Increase in Impermeable Surface, Loss of Evapotranspiration Natural Cooling.

The UHI amplification effects that we consider to dominate listed in the Table are as follows:

- ***The humidity amplification effect:*** This has been observed. For example, Zhao et al. (2014) noted that UHI temperature increases in daytime ΔT by 3.0°C in humid climates but decreasing ΔT by 1.5°C in dry climates. They noted that such relationships imply that UHIs will exacerbate heat wave stress on human health in wet UHI climates. One explanation for this is how heat dissipates through convection which is more difficult in humid climates. Another explanation is that warmer air holds more water vapor. This can increase local specific humidity so that there could be local greenhouse effects.
- ***The heat capacity and solar heating area amplification effect:*** This contributes to the day-night UHI cycle. Here in most cities, it is observed that daytime atmospheric temperatures are actually cooler compared to night. For example, in a study by Basara et al. (2008) in Oklahoma city UHI it was found that at just 9-m height, the UHI was consistently 0.5–1.75°C greater in the urban core than the surrounding rural locations at night. Further, in general UHI impact was strongest during the overnight hours and weakest during the day. This inversion effect can be the results of massive UHI buildings acting like heat sinks, having giant heat capacities and storing heat in their reservoir via convection as solar radiation is absorbed during the day. This often reduces the UHI day effect, but at night buildings cools down, giving off their stored heat that increases local temperatures to the surrounding atmosphere. This effect increases with city growth as buildings have gotten substantially taller (Barr 2019) since 1950.
- ***The Hydro-hotspot amplification effect:*** This effect is not well addressed. Here atmospheric moisture source is a complex issue due to Hydro HotSpots (HHS). Hydro hotspots occur when buildings are hot due to sun exposure. Then during precipitation periods, the hot highly evaporation surfaces increase localized water vapor in the air via the effect that warm air holds more moisture. This increase in local greenhouse gas, could blanket city heat and increase infrared radiation during these periods. This, as discussed above, is another possible UHI humidity amplification.
- ***Reduced Wind Cooling and Solar Canyons:*** In UHIs reduced wind is a known effect due to building wind friction which inhibits cooling by convection. As well, tall buildings create solar canyons and trap sunlight reducing the average albedo although some benefits occurs from shading. In general, both have the effect of amplifying the temperature profile of UHIs.

Data and Methods

We see from the previous section that estimating climate change impact just based on the UHI and Urban area coverage as in Table 1, cannot take into account solar heating building sidewall areas, massive heat capacities, the humidity effects, wind reduction and the solar canyon effect which amplify UHI effects beyond its own climate area.

UHI Area Amplification Factor

In order to estimate the UHI amplification effects, it is logical to first look at UHI footprint (FP) studies as they provide some measurement information. Zhang et al. (2004) found the ecological footprint of urban land cover extends beyond the perimeter of urban areas, and the footprint of urban climates on vegetation phenology they found was 2.4 times the size of the actual urban land cover. In a more recent study by Zhou et al. (2015), they looked at day-night cycles using temperature difference measurements. In this study they found UHI effect decayed exponentially toward rural areas for majority of the 32 Chinese cities. Their study was very thorough and extended over the period from 2003 to 2012. They describe China as an ideal area to study since it has experienced the rapidest urbanization in the world in the decade they evaluated. They found that the “footprint” of UHI effect, including urban areas, was 2.3 and 3.9 times of urban size for the day and night, respectively. We note that the average day-night amplification footprint coverage factor is 3.1.

Looking at Table 2, we see that the UHI Amplification Factor (AF_{UHI}) is highly complex making it difficult to assess from first principles as it would be some function of Table 2 components where

$$AF_{UHI \text{ for } 2019} = f\left(\overline{Build}_{Area} \times \overline{Build}_{C_p} \times \overline{R}_{wind} \times \overline{LossE}_{vtr} \times \overline{Hy} \times \overline{S}_{canyon}\right) \quad (1)$$

where

\overline{Build}_{Area} = Average Building Solar Area

\overline{Build}_{C_p} = Average Building heat capacity

\overline{R}_{wind} = Average City Wind Resistance

\overline{LossE}_{vtr} = Average Loss of Evapotranspiration to natural cooling & Loss of wetland

\overline{Hy} = Average Humidity effect due to hydro-hotspot

\overline{S}_{canyon} = Average Solar Canyon Effect

As a helpful example, one basic formulation that might be suggested is a product of power law average ratios over all urban cities compared to a reference year (1950)

$$AF_{UHI \text{ for } 2019} = \left(\frac{\left(\overline{Build}_{Area}\right)_{2019}}{\left(\overline{Build}_{Area}\right)_{1950}}\right)^{N_1} \left(\frac{\left(\overline{Build}_{C_p}\right)_{2019}}{\left(\overline{Build}_{C_p}\right)_{1950}}\right)^{N_2} \left(\frac{\left(\overline{R}_{wind}\right)_{2019}}{\left(\overline{R}_{wind}\right)_{1950}}\right)^{N_3} \left(\frac{\left(\overline{LossE}_{vtr}\right)_{2019}}{\left(\overline{LossE}_{vtr}\right)_{1950}}\right)^{N_4} \left(\frac{\left(\overline{Hy}\right)_{2019}}{\left(\overline{Hy}\right)_{1950}}\right)^{N_5} \left(\frac{\left(\overline{S}_{canyon}\right)_{2019}}{\left(\overline{S}_{canyon}\right)_{1950}}\right)^{N_6} \quad (2)$$

In order to provide some estimate of this factor, we note that Zhou et al. (2015) found the FP physical area (km^2), correlated tightly and positively with actual urban size having correlation coefficients higher than 79%. This correlation can be used to provide an initial estimate of this complex factor. Area estimates have been obtained in the next Section in Table 3 between 2019 and 1950 time frames. These yield the following results for the Schneider et al. (2009) and the GRUMP 2005 extrapolated area results

$$AF_{UHI \text{ for } 2019} = \frac{\left(\text{Urban Size}\right)_{2019}}{\left(\text{Urban Size}\right)_{1950}} \approx \begin{cases} \left(\frac{\left[\begin{smallmatrix} 0.188 \\ 0.059 \end{smallmatrix}\right]_{2019}}{\left[\begin{smallmatrix} 0.188 \\ 0.059 \end{smallmatrix}\right]_{1950}}\right)_{Schneider} = 3.19 \\ \left(\frac{\left[\begin{smallmatrix} 0.952 \\ 0.316 \end{smallmatrix}\right]_{2019}}{\left[\begin{smallmatrix} 0.952 \\ 0.316 \end{smallmatrix}\right]_{1950}}\right)_{Grump} = 3.0 \end{cases} \quad (3)$$

Between the two studies, the UHI area amplification factor average is 3.1. Coincidentally, this is the same factor observed in the Zhou et al. (2015 study) for the average footprint. This factor may seem high. However, it is likely conservative. There are other effects that would be difficult to assess. For example, increases in global draught due to loss of wet lands, deforestation effects due to urbanization and draught related fires. It could also be important to

factor in changes of other impermeable surfaces since 1950 such as highways, large impermeable surfaces (parking lots and event centers), and so forth.

UHI Dome Amplification Alternate Method

An alternate approach to check the estimate of Equation 3, is to look at the UHI's horizontal extent. Fan et al. (2017) using an energy balance model to obtain the maximum horizontal extent of a heat dome in numerous urban areas found the nighttime extent of 1.5 to 3.5 times the diameter of the city's urban area (2.5 average) and the daytime value of 2.0 to 3.3 (2.65).

Applying this energy method (instead of the area ratio factor in Eq. 3), yields a diameter in 2019 compared to that of 1950 increase of about 1.8. This implies a factor of $2.5 \times 1.8 = 4.5$ higher in the night and $2.65 \times 1.8 = 4.8$ in the day in 1950 (average 4.65). This increase occurring 62.5% of the time according to Fan et al., (where their steady state occurred about 4 hours after sunrise and about 5 hours after sunset) yielding an effective UHI acceleration factor of 2.9. We note this acceleration factor is in good agreement with Equation 3. The fact that it is a bit lower may be because Fan et al. only assessed the steady state region, one would anticipate some increase from the non-steady state period.

Area Extrapolations for 1950 and 2019

In order to assess the urbanized area, (also used in determining the UHI amplification factor ratios above), we need to project the Schneider and GRUMP area estimates down to 1950 and up to 2019. Both use datasets from around 2000 so this is a convenient somewhat middle time-frame. Here we decided to use the world population growth rate (World Bank 2018) which varies by year as shown in Appendix A in Figure A1. We used the average growth rate per ½ decade for iterative projections (that averaged between 1.3% to 1.6% per year).

To justify this we see that Figure A2a illustrates that building material aggregates (USGS 1900-2006) used to build cities and roads correlates well to population growth (US Population Growth 1900-2006).

It is also interesting to note that building materials for cities and roads also correlates well to global warming trends (NASA 1900-2006) shown in Figure A2b.

Column 2 in Table 3 show the projections with the actual year (~2000) data point tabulated value also listed in the table (also see Table 1). The UHI area amplification factor of 3.1 (Column 3) are then applied to Schneider and GRUMP studies shown in Column 4.

Table 3. Extrapolated and amplified urbanized coverage estimates

Year	Urban coverage Percent of Earth	Amplification Factor Effect	Effective Amplification Coverage Area Effect
Schneider Study			
1950	0.059*	1	0.059%
2000-2001	0.0051x29%=0.148		
2019	0.188*	3.1 AF _{UHI} **	0.583%
Worst Case GRUMP Study			
1950	0.316%*	1	0.316%
2000	0.027x29%=0.783%		
2019	0.952%*	3.1 AF _{UHI} **	2.95%

*Growth rate of cities using world population yearly growth rate in Fig A1, **AF_{UHI} is the area amplification factor for 2019 referenced to 1950.

Weighted Amplification Albedo Solar Urbanization (WAASU) Model Overview for 1950 & 2019

The WAASU model is very straightforward; it is based on a global weighted albedo model. The Earth Albedo is given by

$$Earth\ Albedo = \sum_i \{ \% Effective\ Surface\ Area_i \times Surface\ Item\ Albedo_i \} + Cloud\ Area \times Cloud\ Albedo \quad (4)$$

Where the effective surface area is given by

$$Effective\ Surface\ Area = Surface\ Area \times \%Solar\ Irradiance \quad (5)$$

We note that the change in the Earth Albedo over time (from 1950 to 2019), is just a function of the UHI area variation, (when holding all unrelated UHI components fixed), that is

$$\left(\frac{dEA}{dt}\right)_{EA'} = \sum_i \left(Albedo_{UHI} \times Solar\ Irradiance \times \frac{dArea_{UHI}}{dt} \right)_i \quad (6)$$

where EA is the Earth Albedo, and EA' are all other Earth components (and held constant). Although it is possible that the solar irradiance percent changes due to new city locations, in this model we assume it is fixed at 100%. This indicates, for example, even if we were to change the Effective Surface Area of say the Sea Ice component due to the fact that it receives about 40% irradiance compared with other areas and redistributed its radiance (per the Earth's energy budget), it would not affect the overall results when looking at the albedo change from 1950 to 2019. Therefore, the model allows freedom to only work with area coverage changes when focusing on the UHI effect. On the other hand, Sea Ice solar irradiance comes into play when we are considering its effect from 1950 to 2019 (see Appendix C). However, the solar radiation weighting, albedo, and areas for all Earth components are subjected to the constraints below.

Model Constraints

This model is subject to the constraint

$$Total\ Area = \sum_i \{ \%Earth\ Surface\ Areas_i \} + \%Cloud\ Area = 100\% \quad (7)$$

and the normalization constraint for the Earth surface areas (when the UHI area is increased) must then be subject to

$$\sum_i \{ \%Earth\ Surface\ Areas_i \} = 100\% - \%Cloud\ Area \quad (8)$$

To simplify things as much as possible, only five Earth constituents are used: Water, Sea Ice, Land, UHI coverage, and Clouds (where land is its area minus the UHI coverage). These components are fairly easy to estimate and references for their values are provided in Appendix D. Furthermore, we use consistent values found in the IPCC AR5 report (Hartmann et al., 2013) assessment of the Earth's energy budget for solar irradiance. The table below summarizes the constraints from the IPCC values.

Table 4. IPCC Earth energy budget values (Hartmann et al., 2013)

IPCC Item	Incident and Reflected Radiation (W/m ²)	Albedo %	Absorbed (W/m ²)
Earth	100/340	29.4118	240=340x(1-.294)
Atmosphere & Clouds	76/340	22.3529	79*
Earth Surface Albedo	24/340	7.0588	161

*taken as mostly clouds

The fixed components of our model maintain relative consistency from 1950 to 2019. The non-fixed value is the urban coverage as indicated by Equation 6. The only unknown value is the land albedo (minus the UHI coverage) and this value is adjusted to obtain the IPCC global albedo of 29.4118% and its land value of incident/reflected value of 7.0588. These values are used as a 1950 starting point and then the 2019 increase for UHI coverage area is inserted. This increases the Earth's area to greater than 100%. Therefore, renormalization is done per the constraint of Equation 8.

Results and Discussion

Using the extrapolated area coverage in Table 3 with the 3.1 amplification factor applied to the urbanized growth, the resulting global albedo change occurred of 29.3956% in 2019 (Table 5b) compared to the earlier 1950 albedo value of 29.4118% (Table 5a) for the Schneider nominal case. As well, for the GRUMP worst case, the albedo changed from 29.4118% (Table 6a) to 29.3322% (Table 6b) due to the urbanized growth.

As we mentioned earlier, the increases in the solar surface area of the Earth, which will occur with city growth of tall buildings and their solar areas, however comparatively small, requires renormalization in the model of the Earth surface components of the WAASU model (see Appendix B). This is displayed in column 3 in Tables 5b and 6b. While the model is sensitive to urban coverage changes, it works well with renormalization showing a high level of consistency to urban coverage proportionality changes. This is indicated in Table 7 where we find the GRUMP 2019 area sensitivity is 0.0944%Norm Area/(W/m²) (=0.271/2.87) compared with the Schneider area sensitivity of 0.0948 %Norm Area/(W/m²) (=0.055/0.58).

Table 5a. Schneider Results (Albedo=29.4118, 1950)

Surface	Albedo	% Area of Surface	Normalized Earth Area	Weighted Albedo %
	A	B	C=A x B x (1-0.67)	A x C
Sum of Water Type		71		
Sea Ice	0.6	15	4.95	2.970
Water	0.06	56	18.48	1.109
Sum of Land Type		29		
Land - (UHI + Coverage)	0.3118	28.941	9.55053	2.978
UHI + Coverage	0.12	0.059	0.01947	0.002
		Σ=100.000	33.000	7.05882
			Cloud Area	
Clouds	0.3336	67	67	22.35294
Σ Sum Earth %			100.000	
Σ Global Albedo				29.4118

Table 5b. Schneider Results (Albedo=29.3956%, 2019)

Surface	Albedo	Normalized % Surface Area	Normalized Earth Area	Weighted Albedo %
	A	B	C=A x B x (1-0.67)	A x C
Sum of Water Type		70.6298		
Sea Ice	0.6	14.9218	4.924194	2.955
Water	0.06	55.7081	18.383673	1.103
Sum of Land Type		29.37		
Land - (UHI + Coverage)	0.3118	28.79	9.5007	2.962
UHI + Coverage	0.12	0.58	0.1914	0.023
		Σ=100.000	33.000	7.0197
			Cloud Area	
Clouds	0.3336	67	67	22.3529
Σ Sum Earth %			100.000	
Σ Global Albedo				29.3956

Table 6a. GRUMP Results (Albedo=29.4118, 1950)

Surface	Albedo	% Surface Area	Normalized Earth Area	Weighted Albedo %
	A	B	C=A x B x (1-0.67)	A x C
Sum of Water Type		71		
Sea Ice	0.6	15	4.95	2.970
Water	0.06	56	18.48	1.109
Sum of Land Type		29		
Land - (UHI + Coverage)	0.3135	28.684	9.46572	2.968
UHI + Coverage	0.12	0.316	0.10428	0.013
Sum Surface %		Σ=100.000	33.000	7.0588
			Cloud Area	
Clouds	0.3336	67	67	22.3529
Σ Sum Earth %			100.000	
Σ Global Albedo				29.4118

Table 6b. GRUMP Results (Albedo=29.3322%, 2019)

Surface	Albedo	Normalized % Surface Area	Normalized Earth Area	Weighted Albedo %
	A	B	C=A x B x (1-0.67)	A x C
Sum of Water Type		69.1778		
Sea Ice	0.6	14.615	4.82295	2.894
Water	0.06	54.5628	18.005724	1.080
Sum of Land Type		30.8221		
Land - (UHI + Coverage)	0.3135	27.9478	9.222774	2.891
UHI + Coverage	0.12	2.8743	0.948519	0.114
Sum Earth %		Σ=100.000	33.000	6.8655
			Cloud Area	
Clouds	0.3336	67	67	22.3529
Σ Sum Earth %			100.000	
Σ Global Albedo				29.3322

Table 7 provides a summary of albedo changes found in the WASSU model along with the expected solar long wave radiation increase. From the above global WAASU model, the estimates of the Earth’s radiated long wavelength absorption are set equal to the short wave radiation absorption

$$P_{Total}=340 \text{ W/m}^2 (1-\text{Albedo}) \tag{9}$$

Then the change from 1950 to 2019 represents the equivalent increase in long wave radiation is given by

$$\Delta P_{Total}= 340 \text{ W/m}^2 \{(1-\text{Albedo})_{2019}-(1-\text{Albedo})_{1950}\} \tag{10}$$

Results are compiled in Table 7. The table also includes “what if” estimates, if we could change urbanization to be more reflective with cool roofs to reverse the effect. The values here are relative to the conservative UHI amplification values.

Table 7. Albedo and Radiative Increase Model Results with UHI Effective Area

Year	Urban Extent Global Area %	UHI Effective Global Surface % Area	Normalized UHI Effective Global Surface %Area	Albedo Cities	Global Weighted Albedo	$\Delta P_{\text{Total UHI Radiative Increase W/m}^2$ (%GW)*	Sensitivity $\frac{W}{m^2 \text{ } ^\circ K}$	Model Area Sensitivity $\frac{\Delta P_{\text{Total}} (W / m^2)}{\text{Norm } \% \text{ Area}}$
Nominal Case IPCC Schneider 2009 Study								
1950	0.059	0.059	0.059	0.12	29.4118	0	—	—
2019	.188	0.583	0.58	0.12	29.3978	0.055 (1.54%)*	0.058	0.0948
What if	0.188	0.583	0.58	0.204	29.4118	-0.055 (-1.54%)*	-0.058	—
Worst Case GRUMP 2005 Study								
1950	0.316%	0.316	0.316	0.12	29.4118	0	—	—
2019	0.952%	2.95	2.8743	0.12	29.3322	0.271 (7.6%)*	0.285	0.0944
What if	0.952%	2.95	2.8743	0.2039	29.4118	-0.271 (-7.6%)*	-0.285	—

*Percent of Warming estimate, $P=340 \times (1-\text{Albedo})$, $\%GW=\{(P/\varepsilon\sigma)^{0.25}_{2019}- (P/\varepsilon\sigma)^{0.25}_{1950}\}/0.95^\circ\text{C}$, $\varepsilon=1$

The general results are summarized:

- Nominal Schneider case from 1950 to 2019 is 0.055 W/m² due to urban amplification coverage. This would equate to about 1.55% of global warming assuming the total increase from 1950 is about 0.95°C in 2019.
- Worst GRUMP case from 1950 to 2019 is 0.271 W/m² due to urban amplification coverage. This would roughly equate to about 7.5% of global warming assuming the total increase from 1950 is about 0.95°C in 2019.
- “What if” corrective action results of cool roofs indicates that changing city albedos in both the Schneider and the GRUMP case from 0.12 to 0.204 would reverse the increase in emission back to 1950 levels.

Model consistency is indicated in the area sensitivity column in Table 7. Furthermore, we note that radiation increase goes as the area change. That is, the Schneider to Grump normalized area increase from 0.58 (Schneider) to 2.8743% (GRUMP) yields a factor of 3.96 $(=(2.874-.58)/.58)$. This is compared to the observed long radiation increase from 0.055W/M2 (Schneider) to 0.271W/M2 (GRUMP) that also yields a similar factor of 3.93 $(=(0.271-.055)/.055)$. This observation along with the area sensitivity values can be helpful in estimating future warming trends due to UHI growth rates which at the present time from Figure A1 is about 1.2% per year. We also note that in both the Schneider and GRUMP case, implementing cool roof requires the same albedo change from 0.12 to 0.204 in order to reverse the warming trend.

Although global warming assessment obtained in the WAASU model, especially for the Schneider case does not appear to show much contribution to global warming, we find that climate sensitivity estimates could increase this significantly. Suggestions in Appendix D indicate that the root cause global warming contribution may go as high as 5% for the Schneider case and 24% for the GRUMP case (see Table C2).

5. Conclusions

In this paper we were able to estimate using UHI effect (with urban area) amplification coverage estimates with the aid of estimated UHI amplification factors. These estimates inserted into our WAASU model found that between 0.055 and 0.271 W/m² of radiative forcing is possible according the WAASU model (this results indicates that about 1.6 and 7.5% of global warming may be due to the UHI effect (with urban areas). The model found that the effect was proportional to the UHI amplification area coverage with area sensitive estimate was about 0.095 (W/m²)/%Normalized Area. This value could also increase significantly when climate feedbacks are considered (discussed in Appendix C). As area estimates and UHI amplification factors are very sensitive to the final results, it is clear refined values of both would be very helpful.

Although these values appear small, when other climate feedbacks are considered (as in Appendix C) the study points more strongly towards the need for albedo enhancements like cool roofs in cities and urban areas to help stop related global warming anomalies.

Below we provide suggestions and corrective actions which include:

- IPCC to providing albedo guidelines or recommendation similar to their CO2 effort for both UHIs and roads
- A guideline for future albedo design requirements of city and roads should be developed
- Recommend an agency like NASA be tasked with finding applicable solutions to cool down UHIs.
- Recommendation for cars to be more reflective. Here although world-wide cars likely do not embody much of the Earth's area, recommending that all new manufactured cars be higher in reflectivity (e.g., silver or white) would help raise awareness of this issue similar to electric cars that help improve CO2 emissions

Appendix A Growth Rates and Natural Aggregates Information

Below is a plot of the world population growth rate that varies from about 2.1 to 1.1. This is used to make growth rate estimate of urban coverage. We note that natural aggregate used to build cities and roads are reasonably correlated to population growth in Figure A2a. Also of interest (Fig. A2b) is the fact that one can see some correlation to global warming with the use of natural aggregates.

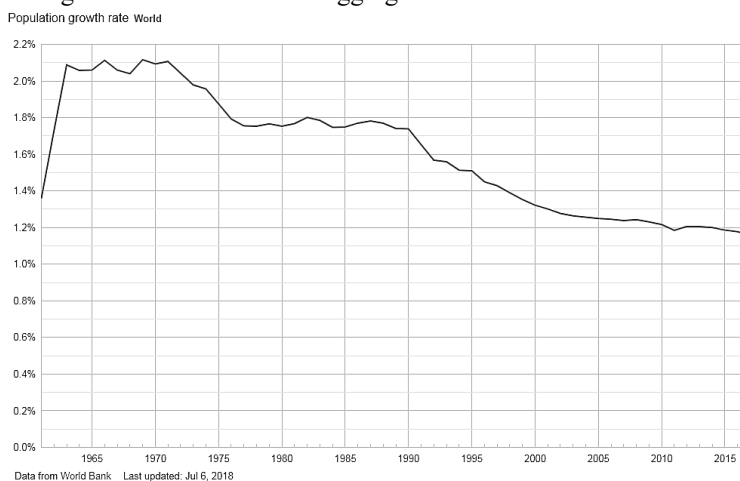


Figure A1 Population growth rate by year from 1960 to 2018, World Bank, 2018

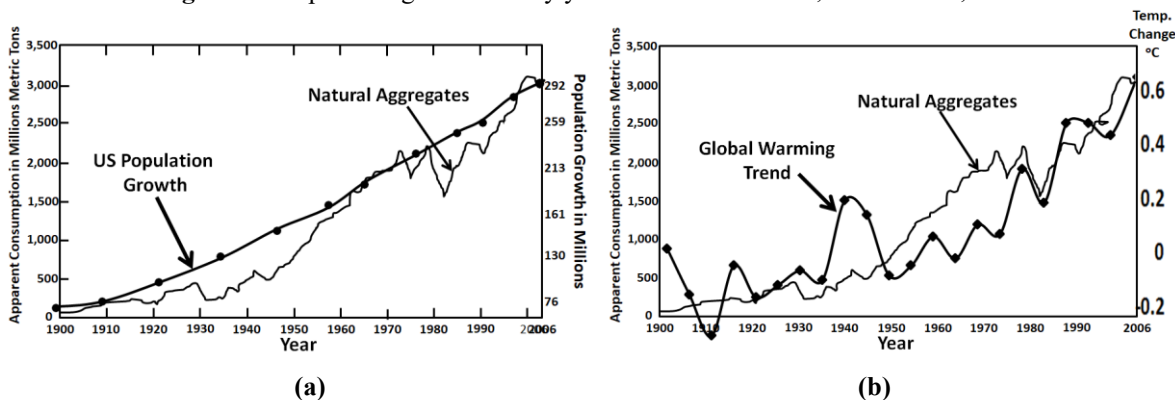


Figure A2 a) Natural aggregates correlated to U.S. Population Growth (USGS 1900-2006) **b)** Natural aggregates correlated to global warming (NASA 2020)

Appendix B: Albedo Model Renormalization Information

Table 5a and b are reproduced to illustrate the renormalization method.

Table 5a. Schneider Results (Albedo=29.4118, 1950)

Surface	Albedo	% Area of Surface	Normalized Earth Area	Weighted Albedo %
	A	B	$C=A \times B \times (1-0.67)$	A x C
Sum of Water Type		71		
Sea Ice	0.6	15	4.95	2.970
Water	0.06	56	18.48	1.109
Sum of Land Type		29		
Land - (UHI + Coverage)	0.3118	28.941	9.55053	2.978
UHI + Coverage	0.12	0.059	0.01947	0.002
		$\Sigma=100.000$	33.000	7.05882
			Cloud Area	
Clouds	0.3336	67	67	22.35294
Σ Sum Earth %			100.000	
Σ Global Albedo				29.4118

Table 5b. Schneider Results (Albedo=29.3956%, 2019)

Surface	Albedo	Normalized % Surface Area	Normalized Earth Area	Weighted Albedo %
	A	B	$C=A \times B \times (1-0.67)$	A x C
Sum of Water Type		70.6298		
Sea Ice	0.6	14.9218	4.924194	2.955
Water	0.06	55.7081	18.383673	1.103
Sum of Land Type		29.37		
Land - (UHI + Coverage)	0.3118	28.79	9.5007	2.962
UHI + Coverage	0.12	0.58	0.1914	0.023
		$\Sigma=100.000$	33.000	7.0197
			Cloud Area	
Clouds	0.3336	67	67	22.3529
Σ Sum Earth %			100.000	
Σ Global Albedo				29.3956

Renormalization is done as follows:

1. Model starts with 1950 Table 5a albedo 29.4118%, then 2019 Urban Coverage area is entered
2. For example, in Table B1, the new area increases from 0.59% to .583%. This is 0.525% larger, now the “Sum of % of Earth Area” will be 100.527% in 2019
3. All areas are renormalized to 101.527%. For example, Sea Ice at 15% in 1950 becomes $15\% \times (100.000/100.527) = 14.921\%$ and the Urban Coverage becomes $0.583\% \times (100/101.11) = 0.58\%$.

Appendix C Related Warming Estimates and Other Amplification Factors

Although UHIs do not appear to contribute much to global warming, when other amplification factors are estimated, more significance can be estimated. In this section, additional factors are suggested providing global warming estimates. Such factors can be contentious; therefore we have chosen to provide these in this appendix mainly as an aid for the reader to illustrate how climate sensitivity can factor into the magnitude of UHIs warming significance.

Global Feedback Amplification Factors

There is a wide range of possible estimates of climate feedback sensitivity driven by uncertainties in how water vapor, clouds, and other factors change as the Earth warms. Climate feedbacks are mixed and some will amplify (positive feedback) or diminish the effect of warming from the root cause effects (see for example Hausfather 2018). The actual feedback is known to be positive (van Nes, 2015). Climatologist will often approximate such factors frequently in reference with CO₂ doubling theory as positive. For example, water-vapor feedback alone, which is one of the most important in our climate system, is thought to have the capacity to about double the direct warming (Manabe and Wetherald, 1967; Randall et al., 2007, Dessler et. Al, 2008). This results from the fact that warm air holds more greenhouse moisture gas. Climate models incorporate this feedback. Water vapor feedback is strongly positive, with most evidence supporting a magnitude of 1.6 to 2.0 W/m²/K (Dessler et. al., 2008). Water vapor feedback is considered a faster feedback mechanism (Hansen, 2008). We will use a factor of 1.75, a bit less than a doubling factor of 2. This factor would apply equally to UHI warming contribution, Greenhouse Gases (GHG), or warming due to Sea Ice melting.

Melting of Sea Ice

While the Antarctic Sea Ice has remained roughly constant, the arctic sea ice is melting at an alarming rate of 12.85% in the last two decades (NASA Sea Ice, 2019). This apparent trend appears yields about a 26% change in sea ice. It is difficult to find a strong reference for estimating global warming impact due to Arctic Sea Ice melting. However, we might get a rough approximation for this using WAASU model (which may illustrate one of the

strengths of the model). Sea Ice melting results in a significant albedo change roughly from Ice albedo of 0.6, to the open ocean albedo of 0.06 (see Table C1 and C2). Fortunately, the Arctic areas receive only about 40% as much solar radiation (Sciencing, 2018). From Equation 5, the effective Sea Ice surface area reduction can be approximated as

$$\text{Effective Sea Ice Surface area} = 15\% (1 - 0.26 \times 0.40) = 13.44\% \text{ (a 1.56\% reduction of effective area)} \quad (\text{C-1})$$

In the WAASU model, we will have to make an assumption that the effective Ocean surface area increases proportionately by 1.56% to 57.56% (see Table C2). The model finds that the Global albedo change decreases from 29.4118% to 28.9948. (Note that alternately we could have set the albedo to 29.4118% in 2019 and worked back to 1950. In this case the albedo would have increase to 29.83%).

Table C1. Schneider Results (Albedo=29.4118, 1950)

Surface	Albedo	% Area of Surface	Normalized Earth Area	Weighted Albedo %
	A	B	C=A x B x (1-0.67)	A x C
Sum of Water Type		71		
Sea Ice	0.6	15	4.95	2.970
Water	0.06	56	18.48	1.109
155Sum of Land Type		29		
Land - (UHI + Coverage)	0.3118	28.941	9.55053	2.978
UHI + Coverage	0.12	0.059	0.01947	0.002
		$\Sigma=100.000$	33.000	7.05882
			Cloud Area	
Clouds	0.3336	67	67	22.35294
Σ Sum Earth %			100.000	
Σ Global Albedo				29.4118

Table C2. Sea Ice Loss Albedo Change (29.0643%, 2019)

Surface	Albedo	Normalized % Surface Area	Normalized Earth Area	Weighted Albedo %
	A	B	C=A x B x (1-0.67)	A x C
Sum of Water Type		71		
Sea Ice	0.6	13.44	4.4352	2.507
Water	0.06	57.56	18.9948	1.14
Sum of Land Type		29	23.43	
Land - (UHI + Coverage)	0.3118	28.941	9.55053	2.978
UHI + Coverage	0.12	0.059	0.01947	0.002
		100.000	33.000	6.6395
			Cloud Area	
Clouds	0.3336	67	67	22.3530
Σ Sum Earth %			123.430	
Σ Global Albedo				29.1338

The Global Warming (GW) is found as

$$\%GW = \{(P/\epsilon\sigma)^{0.25}_{2019} - (P/\epsilon\sigma)^{0.25}_{1950}\} / 0.95^\circ\text{C} \quad (\text{C-2})$$

where $P=340\text{W/m}^2 \times (1-\text{Albedo})$, $\epsilon=1$. The warming increase due to ice melting is estimated from this model to be about 0.25°C or 26.4%.

This estimate is uncertain as climatologist find it hard to know the possible cloud coverage increase from additional warming evaporation. However, one would expect less evaporation in the Arctic. Thus, there are a lot of uncertainties.

Table C3 summarizes the key global warming cause and effect factors that we have described.

Table C3. Global warming factors of interest

Urban Climate Amplification	Effects	Where Applied
UHI Area Amplification Factor	3.1 UHI Amplification	Applied to 2019 UHI Area
UHI Dome Horizontal Method	2.9 UHI Amplification	Applied to 2019 UHI Area
Ice Melting	0.25°C	25°C out of 0.95°C
Atmospheric Moisture Increase	1.75 GW Amplification	Applied to Ice Melting Temp, UHI, and GHGs +X*

where X is any other feedbacks (positive of negative)

Then contributions to global warming can be simplified as follows

$$\Delta T_{GW} = \lambda \Delta F = \Delta T_{UHI} + \Delta T_{Water-Vapor} + \Delta T_{Sea-Ice} + \Delta T_{GHG+X} \quad (\text{C-3})$$

where $\Delta T_{GW}=0.95^{\circ}\text{C}$, $\Delta T_{UHI}=0.0147^{\circ}\text{C}$ (Table 7), $\Delta T_{Sea-Ice}=0.25^{\circ}\text{C}$, λ is the climate sensitivity, and ΔF is the radiative forcing. We have two unknowns $\Delta T_{Water-Vapor}$ and ΔT_{GHG+X} . These may be solved from the following two equations

$$0.95^{\circ}\text{C} = AF_{\text{water vapor}} \times (\Delta T_{UHI} + \Delta T_{GHG+X} + \Delta T_{Sea-Ice}) = 1.75 (0.0147^{\circ}\text{C} + \Delta T_{GHG+X} + 0.25^{\circ}\text{C}) \quad (\text{C-4})$$

and

$$0.95^{\circ}\text{C} = \Delta T_{UHI} + \Delta T_{GHG+X} + \Delta T_{Sea-Ice} + \Delta T_{Water-Vapor} = 0.0147^{\circ}\text{C} + \Delta T_{GHG+X} + 0.25^{\circ}\text{C} + \Delta T_{Water-Vapor} \quad (\text{C-5})$$

The water vapor $AF_{\text{water-vapor}}=1.75$ is discussed above. Then solving, the results are tabulated in the Table C3. We note that in terms of root causes, these suggested values indicate that the UHI effect (with coverage) is responsible for between 5 to 24% of global warming.

Table C3. Global Warming Estimate 2019

Warming Component	Temperature Contribution ($^{\circ}\text{C}$)	Percent of GW Root Cause	Percent of GW	Radiative Forcing W/m^2
Schneider Study				
Urbanization	0.0146	<u>5</u>	1.54	0.055
Greenhouse Gases + X	0.278	95	29.3	1.5
Sea Ice Melting Feedback	0.25		26.3	1.35
Water vapor feedback	0.4073		42.9	2.19
Total	$\Sigma 0.95$			5.1
GRUMP Study				
Urbanization	0.0713	<u>24.4</u>	7.6%	0.271
Greenhouse Gases + X	0.2215	75.6	23	1.19
Sea Ice Melting Feedback	0.25		26	1.25
Water vapor feedback	0.407		43	2.19
Total	$\Sigma 0.95$			4.9

We note from the table that the UHI effect shows a feedback sensitivity of about 3.2 (5%/1.54% or 24%/7.6%). This also indicated that the UHI area sensitivity would increase by 3.3 from 0.094 to about 0.3 $\text{W/m}^2/\%$ Normalized Area (see Table 7).

Often, we would like an estimate of the GHG effect related to CO_2 . If we use a low value for the doubling temperature of 1.5°C then $\lambda_{\text{CO}_2} \approx 0.4^{\circ}\text{C}/(\text{W/m}^2)$. Then solving for forcing we have

$$\Delta T_{\text{CO}_2+X} = \lambda \Delta F = \Delta F (\lambda_{\text{CO}_2} + \lambda_X) = 0.278 = 1.5(0.4 + \lambda_X) \quad (\text{C-6})$$

Results indicate that $\Delta T_{\text{CO}_2} \approx 0.6^{\circ}\text{C}$, $\Delta T_X = -0.32^{\circ}\text{C}$, and $\lambda_X = -0.214$.

Appendix D WAASU Model References

Table D1 provides references for the WAASU model values.

Table D1 Key References for WAASU Model

Parameter	Albedo (reference)	1950 Area (reference)
Sea Ice	50-70%, average 60% (NSID 2020)	15% (Lindsey 2019)
Water	0.06 (NSIDC 2020)	56% Ocean+Sea Ice=71% (USGS)
Land-(UHI+Coverage)	Adjusted to obtain 29.412% and surface reflected of 7.06 Earth Albedo in 1950 thereafter held fixed (see IPCC Hartmann (2013) AR5 report)	29%-Urban Coverage
UHI+Cov	0.12 Sugawara et. Al (2014)	See Table 1
Clouds	22.35294 (IPCC Hartmann et al., 2013)	67% (Earthobservatory, NASA)
Earth Albedo	29.412% (IPCC Hartmann, 2013)	-

References

- Barr J. M., 2019 The Economics of Skyscraper Height (Part IV): Construction Costs Around the World, <https://buildingtheskyline.org/skyscraper-height-iv/>
- Basara J. ,P. Hall Jr. , A.Schroeder , B.Illston ,K.Nemunaitis 2008, Diurnal cycle of the Oklahoma City urban heat island, *J. of Geophysical Research*
- Cao C.X. , Zhao J., P. Gong, G. R. MA, D.M. Bao, K.Tian, Wetland changes and droughts in southwestern China, *Geomatics, Natural Hazards and Risk*, Oct 2011, <https://www.tandfonline.com/doi/full/10.1080/19475705.2011.588253>
- Cormack L. 2015 Where does all the stormwater go after the Sydney weather clears? The Sydney Morning Herald, <https://www.smh.com.au/environment/where-does-all-the-stormwater-go-after-the-sydney-weather-clears-20150430-1mx4ep.html>
- Dessler A. E. ,Zhang Z., Yang P., Water-vapor climate feedback inferred from climate fluctuations, 2003–2008, *Geophysical Research Letters*, (2008), <https://doi.org/10.1029/2008GL035333>
- Earthobservatory, NASA (clouds albedo 0.67) <https://earthobservatory.nasa.gov/images/85843/cloudy-earth>
- Fan, Y., Li, Y., Bejan, A. *et al.* Horizontal extent of the urban heat dome flow. *Sci Rep* 7, 11681 (2017). <https://doi.org/10.1038/s41598-017-09917-4>
- Feddema, J. J., K. W. Oleson, G. B. Bonan, L. O. Mearns, L. E. Buja, G. A. Meehl, and W. M. Washington (2005), The importance of land-cover change in simulating future climates, *Science*, **310**, 1674– 1678, doi:10.1126/science.1118160
- Galka M. 2016, Half the World Lives on 1% of Its Land, Mapped, <https://www.citylab.com/equity/2016/01/half-earth-world-population-land-map/422748/>, (2016 publication on 2000 data set, <http://metrocosm.com/world-population-split-in-half-map/>)
- Global Rural Urban Mapping Project (GRUMP) 2005, Columbia University Socioeconomic Data and Applications Center, Gridded Population of the World and the Global Rural-Urban Mapping Project (GRUMP).
- Hansen, J., "2008: Tipping point: Perspective of a climatologist." Archived 2011-10-22 at the Wayback Machine, Wildlife Conservation Society/Island Press, 2008. Retrieved 2010.
- Hartmann, D.L., A.M.G. Klein Tank, M. Rusticucci, L.V. Alexander, S. Brönnimann, Y. Charabi, F.J. Dentener, E.J. Dlugokencky, D.R. Easterling, A. Kaplan, B.J. Soden, P.W. Thorne, M. Wild and P.M. Zhai, 2013: Observations: Atmosphere and Surface. In: *Climate Change 2013: The Physical Science Basis. Contribution of Working Group I to the Fifth Assessment Report of the Intergovernmental Panel on Climate Change* [Stocker, T.F., D. Qin, G.-K. Plattner, M. Tignor, S.K. Allen, J. Boschung, A. Nauels, Y. Xia, V. Bex and P.M. Midgley (eds.)]. Cambridge University Press, Cambridge, United Kingdom and New York, NY, USA.
- Hirshi M. ,Seneviratne S. , V. Alexandrov, F. Boberg, C. Boroneant, O. Christensen, H. Formayer, B. Orlowsky & P. Stepanek, Observational evidence for soil-moisture impact on hot extremes in Europe, *Nature Geoscience* 4, 17-21 (2011)
- Huang Q. , Lu Y. 2015 Effect of Urban Heat Island on Climate Warming in the Yangtze River Delta Urban Agglomeration in China, *Intern. J. of Environmental Research and Public Health* 12 (8): 8773 (30%)
- Jones, P. D., D. H. Lister, and Q.-X. Li, 2008: Urbanization effects in large-scale temperature records, with an emphasis on China. *J. Geophys. Res.*, 113, D16122, doi: 10.1029/2008JD009916.
- Lindsey R, Scott M., (2019), Climate Change: Arctic Sea Ice Summer Minimum, NOAA Climate.gov, <https://www.climate.gov/news-features/understanding-climate/climate-change-minimum-arctic-sea-ice-extent>
- Manabe, S., and R. T. Wetherald (1967), Thermal equilibrium of atmosphere with a given distribution of relative humidity, *J. Atmos. Sci.*, 24, 241–259.
- McKittrick R. and Michaels J. 2004. A Test of Corrections for Extraneous Signals in Gridded Surface Temperature Data, *Climate Research*
- McKittrick R., Michaels P. 2007 Quantifying the influence of anthropogenic surface processes and inhomogeneities on gridded global climate data, *J. of Geophysical Research-Atmospheres*
- McKittrick Website Describing controversy: <https://www.rossmckittrick.com/temperature-data-quality.html>
- NASA 1900-2006 updated, 2020 <https://climate.nasa.gov/vital-signs/global-temperature/>
- NASA 2000, Gridded population of the world, , <https://sedac.ciesin.columbia.edu/data/set/gpw-v3-population-count/data-download>
- NASA Sea Ice, (2019) <https://climate.nasa.gov/vital-signs/arctic-sea-ice/>
- NSID 2020, National Snow & Ice Data Center, "Thermodynamics: Albedo". [nsidc.org](https://nsidc.org/cryosphere/seaice/processes/albedo.html). Retrieved 14 August 2016. <https://nsidc.org/cryosphere/seaice/processes/albedo.html>
- Randall, D. A. et al. (2007), Climate models and their evaluation, in *Climate Change 2007: The Physical Science Basis. Contributions of Working Group I to the Fourth Assessment Report of the Intergovernmental Panel on Climate Change*, edited by S. Solomon et al., pp. 591–662, Cambridge Univ. Press, Cambridge, U.K.
- Ren, G.; Chu, Z.; Chen, Z.; Ren, Y. 2007 Implications of temporal change in urban heat island intensity observed at Beijing and Wuhan stations. *Geophys. Res. Lett.* , 34, L05711,doi:10.1029/2006GL027927.
- Ren, G.-Y., Z.-Y. Chu, J.-X. Zhou, et al., (2008): Urbanization effects on observed surface air temperature in North China. *J. Climate*, 21, 1333-1348

- Schmidt G. A. 2009 Spurious correlations between recent warming and indices of local economic activity, *Int. J. of Climatology*
- Schneider, A., M. Friedl, and D. Potere, 2009: A new map of global urban extent from MODIS satellite data. *Environmental Research Letters*, 4(4), 044003, doi:10.1088/1748-9326/4/4/044003
- Satterthwaite D.E., F. Aragón-Durand, J. Corfee-Morlot, R.B.R. Kiunsi, M. Pelling, D.C. Roberts, and W. Solecki, 2014: Urban areas. In: *Climate Change 2014: Impacts, Adaptation, and Vulnerability. Part A: Global and Sectoral Aspects. Contribution of Working Group II to the Fifth Assessment Report of the Intergovernmental Panel on Climate Change (IPCC)*
- Sciencing (2018) <https://sciencing.com/sun-intensity-vs-angle-23529.html>
- Stone B. 2009 Land use as climate change mitigation, *Environ. Sci. Technol.*, 43(24), 9052– 9056, doi:10.1021/es902150g
- Sugawara, H., Takamura, T. Surface Albedo in Cities (0.12): Case Study in Sapporo and Tokyo, Japan. *Boundary-Layer Meteorol* **153**, 539–553 (2014). <https://doi.org/10.1007/s10546-014-9952-0>
- US Population Growth 1900-2006, u-s-history.com/pages/h980.html
- USGS 1900-2006, Materials in Use in U.S. Interstate Highways, <https://pubs.usgs.gov/fs/2006/3127/2006-3127.pdf>
- USGS on Amount of Earth covered by water, https://www.usgs.gov/special-topic/water-science-school/science/how-much-water-there-earth?qt-science_center_objects=0#qt-science_center_objects
- van Nes E. H., Scheffer M., Brovkin V., Lenton T. M., Ye H, Deyle E. and Sugihara G., *Nature Climate Change* 2015. [dx.doi.org/10.1038/nclimate2568](https://doi.org/10.1038/nclimate2568)
- World Bank, 2018 population growth rate, worldbank.org
- Yang, X.; Hou, Y.; Chen, B. 2011 Observed surface warming induced by urbanization in east China. *J. Geophys. Res. Atmos*, 116, doi:10.1029/2010JD015452.
- Zhang, X., Friedl, M. A., Schaaf, C. B., Strahler, A. H. & Schneider, A. 2004 The footprint of urban climates on vegetation phenology. *Geophys. Res. Lett.* **31**, L12209
- Zhao, Z.-C., 1991: Temperature change in China for the last 39 years and urban effects. *Meteorological Monthly* (in Chinese), 17(4), 14-17.
- Zhao, Z.-C., 2011: Impacts of urbanization on climate change. in: *10,000 Scientific Difficult Problems: Earth Science*, 10,000 scientific difficult problems Earth Science Committee Eds., Science Press, 843-846. 30%
- Zhao L, Lee X, Smith RB, Oleson K, Strong 2014, contributions of local background climate to urban heat islands, *Nature*. 10;511(7508):216-9. doi: 10.1038/nature13462
- Zhou D. , Zhao S. , L. Zhang, G Sun and Y. Liu, 2015, The footprint of urban heat island effect in China, *Scientific Reports*. 5: 11160
- Zhou Y. , Smith S. , Zhao K. , M. Imhoff, A. Thomson, B. Lamberty, G. Asrar, X. Zhang, C. He and C. Elvidge, A global map of urban extent from nightlights, *Env. Research Letters*, 10 (2015), (study uses a 2000 data set).

Conflicts of Interest

The author declares that he has no conflicts of interest.

Corresponding Author

Alec Feinberg, DfRsoft@gmail.com, 9191-908-9592